Utility of intraoperative near-infrared spectroscopy in the prevention of neurological injury during surgical management of spinal deformity. Preliminary study

Nicolas. Mainard[1], Songlin. Li[2] , Karim. Messaoudene[2], Federico Canavese[1,3], Édouard de Charnacé[4], Raphael. Vialle[5], Sylvain. Feruglio[2]

1Department of Pediatric Surgery, Jeanne-de-Flandre Hospital, CHU Lille, avenue Eugène-Avinée, 59000 Lille, France ; 2Sorbonne University, CNRS UMR7606, Laboratoire d'Informatique de Paris 6 (LIP6), 4 place Jussieu, 75252 PARIS cedex 05, France ; 3University of Lille, 42 Rue Paul Duez, 59000 Lille ; 4Department of Pediatric Surgery, American Memorial Hospital, CHU de Reims, 47 Rue Cognacq Jay - 51090 Reims Cedex, France; 5 Clinical Research Group "RIC" Robotics and Surgical Innovations, GRC-33 Sorbonne University, 26 avenue du Dr. Arnold Netter, 75012 Paris, France.

Corresponding author: Nicolas Mainard, Department of Pediatric Surgery, Jeanne-de-Flandre Hospital, CHU Lille, avenue Eugène-Avinée, 59000 Lille, France. Mail: nicolas.mainard@orange.fr

Abstract - To date, there is no way to directly and locally monitor spinal cord (SC) oxygenation to prevent iatrogenic neurological injury during spine surgery. The aims were to develop and test in vivo on a pig model a prototype to monitor in real time and intraoperatively the oxygenation of the SC using near infrared spectroscopy (NIRS) technology.

Methods: We conducted an animal experiment on a pig. We performed 4 series of measurements. 1-2) Ear and vertebrae of the animal in normal condition (baseline, i.e. without any stimulation); 3-4) Vertebrae after induction of hypoxia and tachycardia.

Results: The use of our probe on the ear and on the vertebra in basic condition allowed us to record heart rate, respiratory rate and local oxygen saturation similar in both cases and comparable to that found on the anesthesia monitor. During hypoxia induction, locally measured oxygen saturation decreases from 100% to 60%. It then increases again when the hypoxia induction sequence is stopped and returns to its baseline value. At the same time, an increase in heart rate was observed in response to hypoxia. After induction of tachycardia by injection of adrenaline, our prototype was able to measure an increase in heart rate of 100 bpm to 200 bpm, comparable to anesthetic monitoring.

Conclusion: We have successfully tested a prototype for real-time monitoring of SC oxygenation in large animals and its ability to detect alterations in SC vascularization and oxygenation. This study attests that NIRS technology is a promising tool for the spine surgeon in the future.

Keywords: spinal cord; Oxygenation; Monitoring; Near infrared spectroscopy; Photoplethysmogram.

I. Introduction

Surgery for idiopathic scoliosis is a common procedure, but remains a demanding surgery for the surgeon, as the impact of neurological complications can be disabling for the patient. During this surgery, the risk of neurological injury is estimated to be from 0.5 to more than 1%, depending on the approach [1,2]. This risk increases in case of fixed thoracolumbar deformation of the sagittal plane [3,4] or in patients at risk, such as early onset scoliosis [5].

To date, there is no way to directly and locally monitor spinal cord (SC) oxygenation to prevent iatrogenic neurological injury. The monitoring of sensory and motor evoked potentials is the reference technique, but it does not always allow the detection of spinal cord suffering during surgery [6,7].

Continuous oxygen saturation monitoring using near infrared spectroscopy (NIRS) is an optical technology for detecting hemodynamic changes in tissue. It has the advantages of being real-time, continuous, inexpensive, portable and non-invasive. It is a simple and widespread tool for monitoring tissue vitality and blood perfusion in many organs [8].

In 2019, a previous experiment allowed us to develop a first prototype of a medical device to monitor in real time and intraoperatively the oxygenation (SpO2) of the SC in large animals using this technology [9].

The aims of this new experiment were to develop and test in vivo on a pig model, this new device following the identification of the limits of the previous experiment, as well as to test its capacity to detect different situations of physiological modifications at the level of the SC.

II. Material and Method

1) NIRS technology

NIRS is based on the principle that body tissues are relatively transparent to light in the near infrared spectral window (650-1000 nm) [10]. This light passing through the tissue is partly absorbed by the pigmented compounds of the blood (chromophores). This results in a partial attenuation of the transmitted light. This attenuation is mainly due to the

hemoglobin in the vessels of the microcirculation, smaller than 1 mm in diameter. In addition, NIRS can differentiate the absorption spectra of the most important blood chromophores, including oxygenated hemoglobin (HbO2), deoxygenated hemoglobin (HHb), methemoglobin (MetHb) and cytochrome aa3 (CCO). We can therefore, through an algorithm based on a modified Beer-Lambert law [11] associated with the knowledge of the molar extinction coefficients of each compound we wish to examine, measure the relative changes in oxygen concentration in the tissue using these chromophores [9].

In 1993, NIRS was approved by the Food and Drug Administration (FDA) for continuous monitoring of brain and somatic tissue oxygenation [12]. It is now a monitoring approach used in clinical routine. However, it is still limited to simple access areas of the body, such as the finger, the ear or the brain [8].

2) *Presentation of the prototype*

The probe has the shape of an industrial compass, whose ends have been adapted to accommodate two parts modeled and then 3D printed (Figure 1).

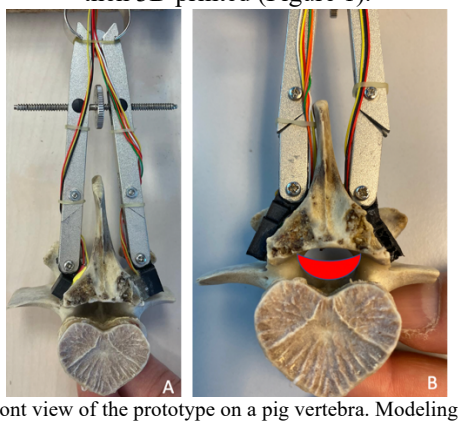

Figure 1. Front view of the prototype on a pig vertebra. Modeling of the light beam on figure 1.B with the "banana" effect allowing to cross an important surface of the SC.

These parts allow to fix on one side, on a 9x9 mm² surface, two chips for the emitting light sources (Figure 2) with 5 different wavelengths (LED USHIO® OPTO SEMICONDUCTOR, INC. SMT735/780/810 and SMT660N/890, respectively for 735, 780, 810, 660 and 890 nm) and a receiver of the other (photodiode with integrated amplifier TSL12S, TAOS®).

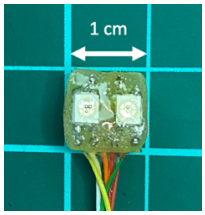

Figure 2. Distal end of the probe with the emitting LEDs (5 wavelengths: 660, 735, 780, 810 and 890 nm).

Both circuits have been coated with transparent epoxy resin, in order to make them perfectly waterproof and resistant to biological liquids. Thanks to 3D printing, an optical mask surrounds the photodetector to limit as much as possible the harmful intervention of the ambient light. This sensor is connected to an Analog to Digital Converter (ADC; ADS 1298, Texas Instruments®) to transform the generated signals into digital data. The acquired signals are called PhotoPlethysmoGrams (PPG). They are the image of blood volume and composition changes in the observation region. The sampling rate of the converter has been set to 100 samples per second for each of the 6 channels (the 5 LEDs and an additional channel to take into account the dark currents and stray lights). The converter interacts, via SPI (Serial Peripheral Interface) communication, with a main board (NRF5340 microcontroller, NORDIC® semiconductor), used to control the entire system and send the acquired data. The ADC-microcontroller association is contained in a waterproof box. It is remote from the operating field via an extension cable which is connected to the probe placed on the monitored area. Finally, the data are sent, via a BLE (Bluetooth Low Energy) communication to another acquisition card to be displayed in real time in the operating room, via a screen and stored in a computer through .CSV files for data backup and post-processing.

3) *Animal experimentation*

We conducted an animal experiment in July 2022, after obtaining authorization from the French Ministry of Research and a favorable evaluation by the Anses/ENVA/UPEC ethics committee.

We chose the pig (Sus scrofa domesticus), because it represented a model relatively close to man in terms of anatomy and vertebral vascularization [13,14]. The animal was a 4 month old pig, weighing approximately 60 kg. A veterinary specialist, was present throughout the procedures. The animal was sedated with isoflurane gas anesthesia (1.5-2% in oxygen/nitrous oxide mixture), and then general anesthesia was maintained with a continuous infusion of propofol [4 ± 6 mg/kg/h]. At the end, the animal was euthanized with an overdose of intravenous Pentobarbital (T61®, embutramide + mebezomium, 11 mL per 60 kg). The respiratory cycle was calibrated to 12-14 cycles per minute, the temperature was maintained at 37° C, and precise monitoring of the animal's vitals was performed throughout the procedure (Vista 120, Dräger ®). The animal was placed in a prone position, allowing a posterior spinal approach freeing the thoracic vertebrae. We performed 4 series of measurements, namely: 1) Ear of the animal in normal condition (baseline, i.e. without any stimulation) (Figure 3); 2) Vertebrae in baseline; 3) Vertebrae after induction of hypoxia; 4) Vertebrae after induction of tachycardia (Figure 4).

No distraction maneuvers or mechanical stimuli will be performed on the animal's spine.

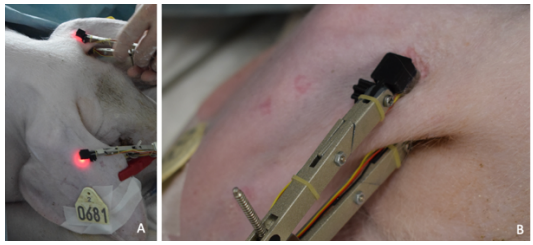

Figure 3 Probes inserted on the animal's ear.

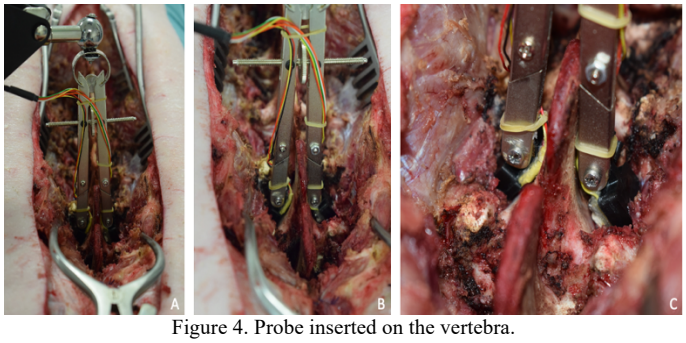

Figure 4. Probe inserted on the vertebra.

III. Results

1) *Comparison of ear and vertebra in normal condition*

Figure 5 shows the results obtained on the ear. Curve 1 shows the PPG curves of the 5 wavelengths after filtering to reduce the level of noise and spurious signals. From Curve 1, we isolate a single PPG, to obtain the peaks, allowing us to recover the heart rate on Curve 3. This one corresponds well to the value displayed on the anesthesia monitor, between 108 and 110 beats per minute (bpm). Curve 4 shows the variations of HbO2, HHb and CCO concentrations. These curves then allow us to reliably estimate SpO2 which oscillates between 98 and 100%. This validates the use of our probe in baseline condition on the ear. All data processing and intermediate steps are detailed in a previous work [9].

Figure 6 shows us, the values recovered in baseline on the vertebra. In the same way, Curve 1 shows us the PPG of the 5 wavelengths. After selecting the peaks (Curve 2), we recover the heart rate which varies around 106 bpm. This time, after an adapted post-processing, we obtain a new curve allowing to isolate again some peaks and thus to estimate the respiratory rate on Curve 5. It varies around 12 breath per minute (Bpm), corresponding to the value of the respiration monitoring. Finally, we recover on Curve 6 the concentrations of the 3 chromophores to obtain on Curve 7, the saturation varying around 99%. These results are coherent and comparable to the values obtained on the animal's ear. The prototype is thus usable on the vertebra in normal condition.

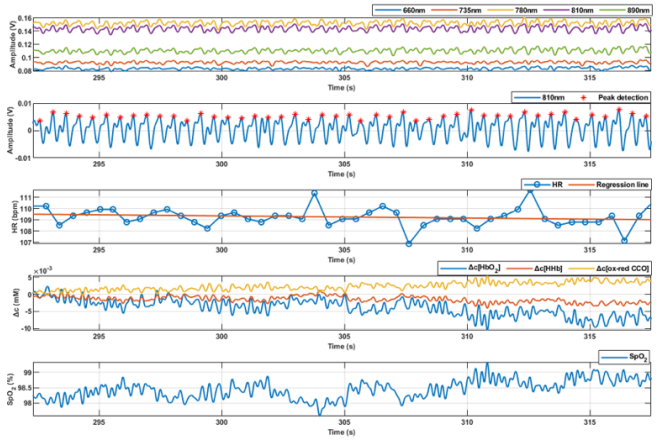

Figure 5. Monitoring obtained on the ear in normal condition. Curve 1: PPG for each wavelength; Curve 2: PPG curve to isolate peaks; Curve 3: Heart rate; Curve 4: Concentration of 3 main chromophores in blood; Curve 4: SpO2 estimation (V: Volts; Bpm: beats per minute; HR: heart rate; nm: nanometer).

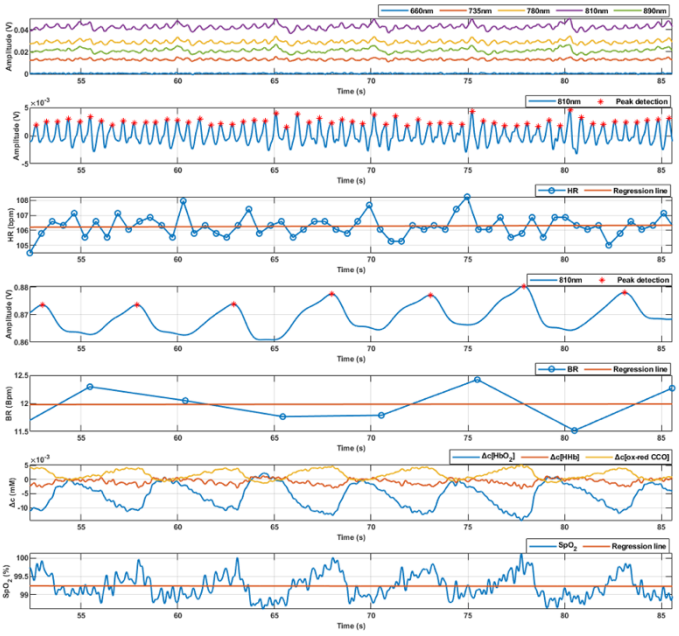

Figure 6. Monitoring obtained on the vertebra in normal condition. Curve 1: PPG for each wavelength; Curve 2: PPG curve to isolate the peaks; Curve 3: Heart rate; Curve 4: PPG curve filtered to isolate the respiratory rate; Curve 5: Respiratory rate; Curve 6: Concentration of the 3 main chromophores in the blood; Curve 7: Estimation of O2 saturation (V: Volts; Bpm: beats per minute; HR: heart rate; BR: breath rate; nm: nanometer).

2) *Vertebrae in hypoxia situation*

We induced hypoxia in the animal by decreasing the respiratory rate associated with a decrease in the fraction of inspired O2, as well as a short curarization of the animal (vecuronium 0.1 mg/kg, IV) (Figure 7).

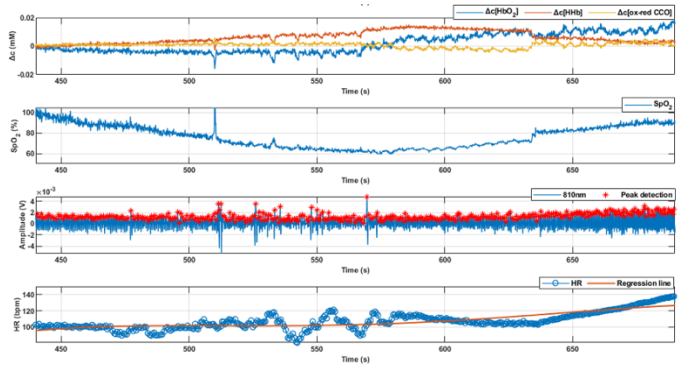

Figure 7. Monitoring obtained on the vertebra during the hypoxia test. Curve 1: Concentration of the 3 chromophores; Curve 2: Estimation of O2 saturation; Curve 3: PPG curve allowing to isolate the peaks; Curve 4: Heart rate.

We can see on Curve 2 that SpO2 starts to decrease steadily from 450 seconds (when the hypoxia phase was initiated), going from 100% to 60%. Then, it rises again when the hypoxia induction sequence is stopped and returns to its baseline value. At the same time, an increase in heart rate is observed on Curve 4, in response to hypoxia. Our prototype thus allowed us to successfully describe a situation of general hypoxia observed on the SC.

3) VERTEBRAE AFTER INDUCTION OF TACHYCARDIA

Next, we induced tachycardia by injection of 20 µg of adrenaline (starting at 300 s; Figure 8).

According to the same principle, from curve 2 representing the concentrations of the different forms of hemoglobin over time, we derive the PPG and after isolating the peaks, we obtain on Curve 3, an acceleration of the heart rate from the basic value around 100 bpm to nearly 200 bpm, which corresponds to the measurements on the anesthesia equipment. At the same time, we observe a slight decrease of SpO2, during the peak of tachycardia, certainly corresponding to a slight peripheral vasoconstriction consecutive to the injection of adrenalin which will spontaneously return to normal afterwards.

We have thus shown that our prototype can effectively detect local hemodynamic variations.

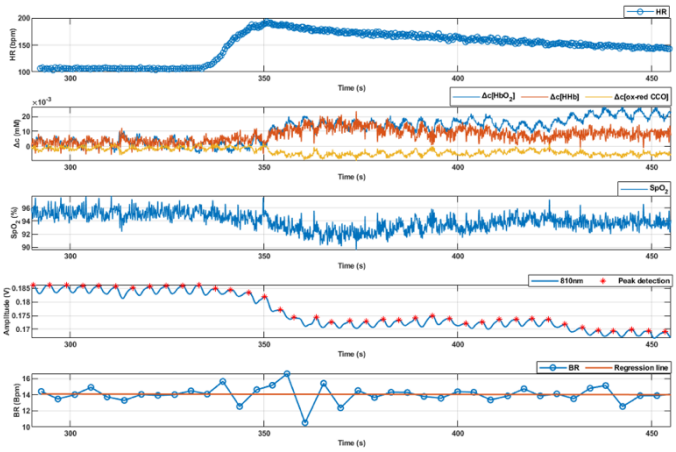

Figure 8. Monitoring obtained on the vertebra during the tachycardia test. Curve 1: Heart rate; Curve 2: Concentration of the 3 main chromophores of the blood; Curve 3: Estimation of O2 saturation; Curve 4: PPG curve filtered to isolate the respiratory rate; Curve 5: Respiratory rate.

IV. DISCUSSION

This study successfully demonstrated the feasibility of a prototype allowing real-time monitoring of hemodynamic variations and, more particularly, SC oxygenation in large animals, as well as its capacity to detect local alterations of vascularization and oxygenation. The design chosen corresponded to the surgical requirements, allowing to have a simple prototype to use in real conditions (i.e., spine surgery) We were able to extract precise local hemodynamic parameters (e.g., heart rate, SpO2, respiratory rate), thanks to the systems developed.

The surgical management of a spinal deformity can be a source of numerous spinal cord injuries. Indeed, the distraction mechanism necessary to reduce the deformity can lead to spasm of the micro-vascularization and intrinsic vascularization of the SC, causing a decrease in spinal cord perfusion. In a second step, the increase in distraction stress may reach the extrinsic vasculature, further reducing the local blood supply and leading to ischemic injury of the SC [15–17]. It is at this moment that a generalized hypotension can occur, visible to the anesthesiologist when monitoring the patient's vitals. Only afterwards does an alteration of the motor and sensory evoked potentials occur. The vascular damage thus precedes the spinal cord injury and its neurological repercussions [18,19]. A device adapted to intraoperative constraints, allowing real-time monitoring of local dynamic changes in the vascularization, would allow the surgeon to adapt his action before the appearance of a neurological lesion. The neurophysiology techniques routinely available during spinal surgery provide essential, but delayed and indirect information on the viability of the SC, making multimodal monitoring essential [20,21]. Available imaging techniques, such as magnetic resonance imaging, considered the gold standard for evaluating all lesions

associated with spinal trauma [22], are not yet available in routine practice. Some invasive options are being developed, such as the insertion of epidural or intrathecal pressure monitoring devices, to better understand the mechanisms of SC perfusion [23, 24].

Despite the relative success of NIRS technology in brain monitoring in traumatic injuries [25], its use in SC remains limited. A systematic review of the literature in 2019 found 26 articles interested in monitoring SC vascularization in humans (n = 9) or animals (n = 17), with optimistic results [27]. Shadgan et al. used NIRS technology to monitor SC oxygenation in a porcine model of acute SC injury and showed that the measured values were highly correlated with intra-parenchymal measures of tissue oxygenation, particularly during periods of hypoxia or altered arterial pressure [26]. These results are found in our study in both conditions.

Human studies use transcutaneous devices applied to the spinal column during surgeries at risk of spinal cord injury such as large aortic trunk surgery [27,28]. They are based on the "paraspinal collateral network" theory, which states that the vascularization of the SC is provided by a network of paraspinal arterial collaterals, shared with the surrounding tissues, including the paraspinal muscles. At present, the results are rather heterogeneous and although there may be a correlation, the authors agree that this is an important delay and that further research and experimentation is needed [9]. The small diameter of the SC and the depth of the underlying tissue make it difficult to assess SC perfusion without a direct surgical approach. In the case of deformity surgery, the surgical approach allows the probe to be placed directly in contact with the posterior lamina. In addition, the small size of the tip of our probe (Figure 1 and 2) would allow it to be placed in contact with the posterior lamina with the surgical material necessary for posterior spinal instrumentation in place. In the case of a laminectomy, if it is necessary, the probe could be placed directly in contact with the SC.

We chose to keep 5 emitting wavelengths to monitor the different chromophores of the blood. The objective was to have as many measurements as possible, in order to better refine our measured values at the cost of a larger footprint. Conventional pulse oximeters use, in most cases, only two lengths and manage to provide a relatively reliable estimate of O2 saturation, while accepting a certain error rate in the accuracy of the measurement (2 to 3% between for a SpO2 between 70 and 100%). It is a question of making a compromise between power and increase of local heat, in order to avoid any iatrogenic lesion of the marrow.

We have chosen to have a probe that monitors only one level at a time. It could be attached directly to the vertebra or held by hand by the operating assistant. It could be moved to the risk areas during spinal deformity surgery (apex of the deformity during reduction or stage after stage during vertebra instrumentation). It could also be used to localize the exact level of spinal cord injury after an evoked potential alert during spine deformity surgery. It could be discussed the possibility of continuous monitoring of the whole spine throughout the operation by changing the conformation of the prototype as it can be done when using NIRS on the skin in front of the spine for the monitoring of the "paraspinal collateral network" during aortic or heart surgery for example [27–29].

This prototype has some limitations and needs to be improved in order to meet the requirements for use in humans. In order to improve the reproducibility of the measurements, we had chosen to fix the probes by means of an articulated arm fixed to the table. This fixation system was incompatible with the respiratory movements of the animal, obliging us to maintain the probes in permanent manual contact with the bone and marrow, which is not viable in a real-life application for the surgeon.

We tested the use of the equipment in baseline condition and after systemic alteration of the circulation. We did not perform any distraction or mechanical stimuli of the spine. It will now be necessary to test its capacity to detect localized alterations of the spinal cord vascularization during subsequent experiments. Moreover, it would be relevant to compare its use to the gold standard, which is currently electro neurophysiology, especially concerning the early detection of lesions.

V. Conclusion and Perspectives

We have successfully tested a prototype for real-time monitoring of SC oxygenation in large animals and its ability to detect alterations in SC vascularization and oxygenation. These preliminary results confirm the optimism created by the first series of experiments. Although this device requires improvement, as well as further rounds of testing under conditions even closer to its future use, this study attests that NIRS technology is a promising tool for the spine surgeon in the future.

References

[1] Coe JD, Arlet V, Donaldson W, et al (2006) Complications in spinal fusion for adolescent idiopathic scoliosis in the new millennium. A report of the Scoliosis Research Society Morbidity and Mortality Committee. Spine (Phila Pa 1976). https://doi.org/10.1097/01.brs.0000197188.76369.13

[2] Diab M, Smith AR, Kuklo TR, et al (2007) Neural complications in the surgical treatment of adolescent idiopathic scoliosis. Spine (Phila Pa 1976). https://doi.org/10.1097/BRS.0b013e31815a5970

[3] Bivona LJ, France J, Daly-Seiler CS, et al (2022) Spinal deformity surgery is accompanied by serious complications: report from the Morbidity and Mortality Database of the Scoliosis Research Society from 2013 to 2020. Spine Deform. https://doi.org/10.1007/s43390-022-00548-y

[4] Smith JS, Sansur CA, Donaldson WF, et al (2011) Short-term morbidity and mortality associated with correction of thoracolumbar fixed sagittal plane deformity: a report from the Scoliosis Research Society Morbidity and Mortality Committee. Spine (Phila Pa 1976). https://doi.org/10.1097/BRS.0b013e3181eabb26

[5] Upasani VV, Parvaresh KC, Pawelek JB, et al (2016) Age at Initiation and Deformity Magnitude Influence Complication Rates of Surgical Treatment With Traditional Growing Rods in Early-Onset Scoliosis. Spine Deform. https://doi.org/10.1016/j.jspd.2016.04.002

[6] Neira VM, Ghaffari K, Bulusu S, et al (2016) Diagnostic Accuracy of Neuromonitoring for Identification of New Neurologic Deficits in Pediatric Spinal Fusion Surgery. Anesth Analg.
https://doi.org/10.1213/ANE.0000000000001503
[7] Thirumala PD, Crammond DJ, Loke YK, et al (2017) Diagnostic accuracy of motor evoked potentials to detect neurological deficit during idiopathic scoliosis correction: a systematic review. J Neurosurg Spine.
https://doi.org/10.3171/2015.7.SPINE15466
[8] Ferrari M, Quaresima V (2012) A brief review on the history of human functional near-infrared spectroscopy (fNIRS) development and fields of application. Neuroimage.
https://doi.org/10.1016/j.neuroimage.2012.03.049
[9] Mainard N, Tsiakaka O, Li S, et al (2022) Intraoperative Optical Monitoring of Spinal Cord Hemodynamics Using Multiwavelength Imaging System. Sensors (Basel).
https://doi.org/10.3390/s22103840
[10] Jöbsis FF (1977) Noninvasive, Infrared Monitoring of Cerebral and Myocardial Oxygen Sufficiency and Circulatory Parameters. Science.
https://doi.org/10.1126/science.929199
[11] Oshina I, Spigulis J (2021) Beer-Lambert law for optical tissue diagnostics: current state of the art and the main limitations. J Biomed Opt.
https://doi.org/10.1117/1.JBO.26.10.100901
[12] Murkin JM, Arango M (2009) Near-infrared spectroscopy as an index of brain and tissue oxygenation. British Journal of Anaesthesia.
https://doi.org/10.1093/bja/aep299
[13] Strauch JT, Lauten A, Zhang N, et al (2007) Anatomy of spinal cord blood supply in the pig. Ann Thorac Surg.
https://doi.org/10.1016/j.athoracsur.2007.01.060
[14] Toossi A, Bergin B, Marefatallah M, et al (2021) Comparative neuroanatomy of the lumbosacral spinal cord of the rat, cat, pig, monkey, and human. Sci Rep.
https://doi.org/10.1038/s41598-021-81371-9
[15] Wu D, Zheng C, Wu J, Xue J, Huang R, Wu D, et al (2017) The pathologic mechanisms underlying lumbar distraction spinal cord injury in rabbits. Spine J.
https://doi.org/10.1016/j.spinee.2017.05.024
[16] Cusick JF, Myklebust J, Zyvoloski M, et al (1982) Effects of vertebral column distraction in the monkey. J Neurosurg.
https://doi.org/10.3171/jns.1982.57.5.0651
[17] Martirosyan NL, Feuerstein JS, Theodore N, et al (2011) Blood supply and vascular reactivity of the spinal cord under normal and pathological conditions. J Neurosurg Spine.
https://doi.org/10.3171/2011.4.SPINE10543
[18] Dolan EJ, Transfeldt EE, Tator CH, et al (1980) The effect of spinal distraction on regional spinal cord blood flow in cats. J Neurosurg.
https://doi.org/10.3171/jns.1980.53.6.0756
[19] Seyal M, Mull B (2002) Mechanisms of signal change during intraoperative somatosensory evoked potential monitoring of the spinal cord. J Clin Neurophysiol. https://doi.org/10.1097/00004691-200210000-00004
[20] Bhagat S, Durst A, Grover H, et al (2015) An evaluation of multimodal spinal cord monitoring in scoliosis surgery: a single centre experience of 354 operations. Eur Spine J.
https://doi.org/10.1007/s00586-015-3766-8
[21] Feng B, Qiu G, Shen J, et al (2012) Impact of multimodal intraoperative monitoring during surgery for spine deformity and potential risk factors for neurological monitoring changes. J Spinal Disord Tech.
https://doi.org/10.1097/BSD.0b013e31824d2a2f
[22] Freund P, Seif M, Weiskopf N, et al (2019) MRI in traumatic spinal cord injury: from clinical assessment to neuroimaging biomarkers. Lancet Neurol.
https://doi.org/10.1016/S1474-4422(19)30138-3
[23] Phang I, Zoumprouli A, Saadoun S, et al (2016) Safety profile and probe placement accuracy of intraspinal pressure monitoring for traumatic spinal cord injury: Injured Spinal Cord Pressure Evaluation study. J Neurosurg Spine 2016;25:398–405. https://doi.org/10.3171/2016.1.SPINE151317
[24] Werndle MC, Saadoun S, Phang I, et al (2014) Monitoring of spinal cord perfusion pressure in acute spinal cord injury: initial findings of the injured spinal cord pressure evaluation study. Crit Care Med.
https://doi.org/10.1097/CCM.0000000000000028
[25] Roldán M, Kyriacou PA (2021) Near-Infrared Spectroscopy (NIRS) in Traumatic Brain Injury (TBI). Sensors (Basel).
https://doi.org/10.3390/s21051586
[26] Shadgan B, Macnab A, Fong A, et al (2019) Optical Assessment of Spinal Cord Tissue Oxygenation Using a Miniaturized Near Infrared Spectroscopy Sensor. J Neurotrauma.
https://doi.org/10.1089/neu.2018.6208
[27] Berens RJ, Stuth EA, Robertson FA, et al (2006) Near infrared spectroscopy monitoring during pediatric aortic coarctation repair. Paediatr Anaesth.
https://doi.org/10.1111/j.1460-9592.2006.01956.x
[28] Badner NH, Nicolaou G, Clarke CFM, et al (2011) Use of Spinal Near-Infrared Spectroscopy for Monitoring Spinal Cord Perfusion During Endovascular Thoracic Aortic Repairs. J Cardiothorac Vasc Anesth.
https://doi.org/10.1053/j.jvca.2010.01.011
[29] von Aspern K, Haunschild J, Khachatryan Z, et al (2022) Mapping the collateral network: Optimal near-infrared spectroscopy optode placement. J Thorac Cardiovasc Surg.
https://doi.org/10.1016/j.jtcvs.2020.07.103